Catastrophic rearrangement of a compact star due to the quark core formation

I.N. Mishustin[1,2,3], M. Hanauske[1], A. Bhattacharyya[1,4], L.M. Satarov[1,2], H. Stöcker[1], and W. Greiner[1]

[1] *Institut für Theoretische Physik, J.W. Goethe–Universität, D–60054 Frankfurt am Main, Germany*
[2] *The Kurchatov Institute, Russian Research Center, 123182 Moscow, Russia*
[3] *The Niels Bohr Institute, DK-2100 Copenhagen Ø, Denmark*
[4] *Scottish Church College, 1&3 Urquhart Square, 700 006 Calcutta, India*

Abstract

We study properties of compact stars with the deconfinement phase transition in their interiors. The equation of state of cold baryon-rich matter is constructed by combining a relativistic mean-field model for the hadronic phase and the MIT Bag model for the deconfined phase. In a narrow parameter range two sequences of compact stars (twin stars), which differ by the size of the quark core, have been found. We demonstrate the possibility of a rapid transition between the twin stars with the energy release of about 10^{52} ergs. This transition should be accompanied by the prompt neutrino burst and the delayed gamma-ray burst.

PACS: 14.65.-q, 26.60.+c, 97.10.-q, 98.70.Rz

1 Introduction

Our main goal in this paper is to study properties of compact stars composed of strongly interacting matter undergoing the deconfinement phase transition. We construct the equation of state (EoS) at finite baryon density ρ_B by combining two popular models of the baryon-rich matter. For the hadronic phase we use the NLZ version of the relativistic mean-field model [1] which gives very good description of the saturation properties of cold nuclear matter. The deconfined phase is described within a simplified version of the MIT Bag model [2]. The possibility of a phase transition between these two phases has been carefully studied by applying the Gibbs conditions for charge-neutral and β-equilibrated matter. Indeed, we have found a first order phase transition and determined characteristics of the mixed phase.

Properties of hybrid stars containing both the hadrons and quarks have been already studied by using a large number of models (see e.g. Refs. [3, 4, 5, 6, 7]). One may wonder, what is new in our work? First of all, we want to note that this paper presents only a

small part of our more comprehensive study [8] where we systematically analyze many other models of hadronic and quark phases. It is interesting that in most cases we do not find any phase transition between the two phases. The combination of the NLZ and MIT Bag models represents one of a few exceptional cases, when the deconfinement phase transition is predicted in stellar interiors. Moreover, we find two families of compact stars, twin stars [9, 10, 11], which differ by the size of the quark core. This opens the possibility of a catastrophic rearrangement of the twin star from one to the other configuration with a release of energy of about 10^{52} erg. In this paper we present these results and discuss their observational consequences.

2 Properties of matter in compact stars

2.1 Hadronic phase

There is no doubt that hadrons, mesons and baryons, are correct degrees of freedom for modeling strongly-interacting matter at low densities. From nuclear phenomenology we know that atomic nuclei can be well described in terms of interacting nucleons. Therefore, we believe that the hadronic phase should be stable at least up to the saturation density of nuclear matter $\rho_0 = 0.15\,\mathrm{fm}^{-3}$. Field-theoretical models, where nucleons interact with mean meson fields, are proved to be very successful in describing saturation properties of nuclear matter as well as properties of finite nuclei. Here, to calculate the EoS of hadronic matter we use a non-linear version of the relativistic mean-field model known as the NLZ model [1]. Compared wih the original version it is generalized by including hyperons (Y) and hyperon-hyperon (YY) interactions, as proposed in Ref. [12]. We call this model NLZY.

The original Lagrangian density for the NLZ model (without the YY interaction) can be written as [1] (here and below we use the units $\hbar = c = 1$)

$$\begin{aligned}\mathcal{L} &= \sum_B \overline{\psi}_B \left(i\partial\!\!\!/ - m_B\right)\psi_B + \frac{1}{2}\partial^\mu\sigma\partial_\mu\sigma - \frac{1}{2}m_\sigma^2\sigma^2 - \frac{a}{3}\sigma^3 - \frac{b}{4}\sigma^4 - \frac{1}{4}\omega^{\mu\nu}\omega_{\mu\nu} + \frac{1}{2}m_\omega^2\omega^\mu\omega_\mu \\ &- \frac{1}{4}\vec{\rho}^{\mu\nu}\vec{\rho}_{\mu\nu} + \frac{1}{2}m_\rho^2\vec{\rho}^\mu\vec{\rho}_\mu + \sum_B \overline{\psi}_B \left(g_{\sigma B}\sigma + g_{\omega B}\omega^\mu\gamma_\mu + g_\rho\vec{\rho}^\mu\gamma_\mu\vec{\tau}_B\right)\psi_B\,, \qquad (1)\end{aligned}$$

where the sum runs over all the baryons B=$p, n, \Lambda, \Sigma^{0,\pm}, \Xi^{0,-}$. In the above Lagrangian σ, ω and $\vec{\rho}$ are the iso-scalar scalar σ, the iso-scalar vector ω and the isovector vector ρ meson fields respectively. In Eq. (1) $\omega^{\mu\nu}$ and $\vec{\rho}^{\mu\nu}$ denote, respectively, the field strength tensors for the ω and ρ meson fields.

Originally this model was designed for the nucleonic sector and it failed to reproduce the observed strong $\Lambda\Lambda$ attractive interaction. This defect can be removed by adding

two new meson fields with hidden strangeness, namely, the iso-scalar scalar σ^* and the iso-vector vector ϕ, which couple to hyperons only [12]. These fields can be identified with the $f_0(975)$ and $\phi(1020)$ mesons. The corresponding Lagrangian is given by

$$\mathcal{L}^{YY} = \frac{1}{2}\left(\partial^\mu\sigma^*\partial_\mu\sigma^* - m_{\sigma^*}^2\sigma^{*2}\right) - \frac{1}{4}\phi^{\mu\nu}\phi_{\mu\nu} + \frac{1}{2}m_\phi^2\phi^\mu\phi_\mu + \sum_Y \overline{\psi}_Y\left(g_{\sigma^*Y}\sigma^* + g_{\phi Y}\phi^\mu\gamma_\mu\right)\psi_Y$$

where index Y runs over hyperons only. The mean meson fields are found from the Euler-Lagrange equations.

The nucleon coupling constants are chosen from the fit of the finite nuclei properties. The vector coupling constants of the hyperons are chosen according to the SU(6) symmetry and the hyperonic scalar coupling constants are chosen to reproduce the measured values of the corresponding optical potentials. Below we use the set of model parameters suggested in Refs. [1, 12].

Within the mean-field approximation, the pressure and energy density of static and homogeneous baryonic matter can be easily calculated from the above Lagrangian:

$$\begin{aligned}\epsilon^H &= \frac{1}{2}m_\sigma^2\sigma^2 + \frac{b}{3}\sigma^3 + \frac{c}{4}\sigma^4 + \frac{1}{2}m_{\sigma^*}^2\sigma^{*2} + \frac{1}{2}m_\omega^2\omega_0^2 + \\ &\quad + \frac{1}{2}m_\rho^2\rho_{0,0}^2 + \frac{1}{2}m_\phi^2\phi_0^2 + \sum_B \frac{\nu_B}{2\pi^2}\int_0^{k_F^B} dk\, k^2\sqrt{k^2 + {m_B^*}^2}\,, \qquad (2)\\ P^H &= -\frac{1}{2}m_\sigma^2\sigma^2 - \frac{b}{3}\sigma^3 - \frac{c}{4}\sigma^4 - \frac{1}{2}m_{\sigma^*}^2\sigma^{*2} + \frac{1}{2}m_\omega^2\omega_0^2 + \\ &\quad + \frac{1}{2}m_\rho^2\rho_{0,0}^2 + \frac{1}{2}m_\phi^2\phi_0^2 + \sum_B \frac{\nu_B}{6\pi^2}\int_0^{k_F^B} dk \frac{k^4}{\sqrt{k^2 + {m_B^*}^2}}\,, \qquad (3)\end{aligned}$$

where $m_B^* = m_B - g_{\sigma B}\sigma - g_{\sigma^* B}\sigma^*$ is the effective mass, ν_B is the degeneracy factor and $k_F^B = \sqrt{\mu_B^2 - {m^*}_B^2}$ is the Fermi momentum of the baryon species B.

In order to have a complete description of the β-equilibrated matter one should also include the leptons. In both the hadronic and quark phases their contributions to energy density and pressure are given by the well known formulae of ideal Fermi gas.

2.2 Deconfined phase

As follows from a simple geometrical consideration, nucleons begin to overlap at densities $\rho_B \sim (4\pi r_N^3/3)^{-1} \simeq 3\rho_0$ for the nucleon radius $r_N \simeq 0.8$ fm. Such densities are surely reached in the interiors of compact stars. Of course, this argument does not tell anything about the character of transition from hadronic to quark-gluon degrees of freedom. Below we follow the common practice of using two different models for these two phases. Namely, the deconfined phase is described within a simple version of the MIT Bag model [2], considering it as a mixture of free Fermi gases of u, d, s quarks in a bag with an additional

energy density B (the bag constant). Within this model the energy density and pressure of cold deconfined matter are written as

$$\epsilon^Q = \sum_{f=u,d,s} \frac{\nu_f}{2\pi^2} \int_0^{k_F^f} dk k^2 \sqrt{m_f^2 + k^2} + B \,, \tag{4}$$

$$P^Q = \sum_{f=u,d,s} \frac{\nu_f}{6\pi^2} \int_0^{k_F^f} dk \frac{k^4}{\sqrt{m_f^2 + k^2}} - B \,, \tag{5}$$

where $k_F^f = \sqrt{\mu_f^2 - m_f^2}$ is the Fermi momentum of quarks with flavor f. For each flavor we choose the degeneracy factor $\nu_f = 2\,(\text{spin}) \times 3\,(\text{color}) = 6$ and take the following values of quark masses: $m_u = 5$ MeV, $m_d = 10$ MeV and $m_s = 150$ MeV.

2.3 Conditions of local equilibrium

In β-equilibrium, the chemical potential of any particle species i can be expressed as

$$\mu_i = b_i \mu_b + q_i \mu_e \ , \tag{6}$$

where b_i is the baryon number of the species i, q_i denotes its charge in units of the electron charge, μ_b and μ_e are the baryonic and electric chemical potentials, respectively. Here and below we assume that neutrinos can freely escape from the star. Eq. (6) means that only reactions conserving charge and baryon number are allowed. On the other hand, strangeness is not conserved because strangeness-changing reactions are generally much faster than a characteristic time of the star evolution. Two independent chemical potentials, μ_b and μ_e, are found by fixing the baryon and electric charge densities:

$$\rho_B = \sum_i b_i \rho_i \,, \qquad \rho_e = \sum_i q_i \rho_i \,, \tag{7}$$

where ρ_i is the number density of the particle species i. It is obvious that stars must be electrically neutral on a macroscopic scale, i.e. $\rho_e = 0$.

We assume that deconfinement is a first order phase transition which, in general, should produce a mixed phase (MP) between the pure hadronic phase (HP) and pure quark phase (QP). At zero temperature the MP should follow the Gibbs conditions

$$P^H(\mu_b, \mu_e) = P^Q(\mu_b, \mu_e) \,, \tag{8}$$

$$\mu_b = \mu_b^H = \mu_b^Q \,, \tag{9}$$

$$\mu_e = \mu_e^H = \mu_e^Q \,. \tag{10}$$

According to Eq. (6), the baryon chemical potential μ_b equals the neutron chemical potential μ_n and μ_e is equal to the electron chemical potential. At given μ_b and μ_e,

the quark chemical potentials are found by using the formulae $\mu_u = (\mu_b - 2\mu_e)/3$ and $\mu_d = \mu_s = (\mu_b + \mu_e)/3$.

The volume averaged energy density in the MP can be written as

$$\epsilon \;=\; (1-\lambda)\epsilon^H(\mu_b,\mu_e) + \lambda\epsilon^Q(\mu_b,\mu_e)\,, \tag{11}$$

where $\lambda = V_Q/V$ is the volume fraction of quark phase. In the case of two chemical potentials one can only construct the MP by adopting a generalized (global) charge neutrality condition [13], when the net positive charge of one phase is compensated by the negative charge of the other phase:

$$(1-\lambda)\rho_e^H(\mu_b,\mu_e) + \lambda\rho_e^Q(\mu_b,\mu_e) = 0\,. \tag{12}$$

This condition is assumed in our calculations of hybrid stars presented below.

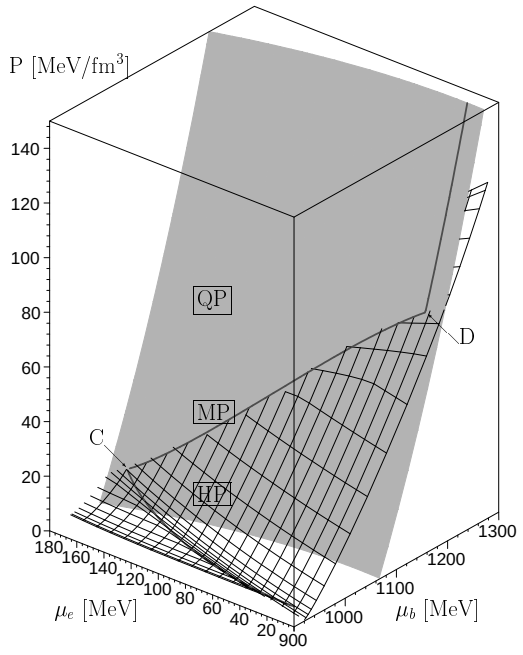

Figure 1: Pressure as a function of μ_b and μ_e for the hadronic phase (wired surface) as predicted by the NLZY model and for the quark phase (grey surface) as predicted by the MIT Bag model ($B^{1/4} = 180$ MeV). The thick line represents the charge neutral matter. Its portion between points C and D corresponds to the mixed phase.

2.4 EoS and composition of matter

Figure 1 shows the pressure surfaces for the pure HP and pure QP (for bag constant $B^{1/4} = 180$ MeV) as functions of chemical potentials μ_b and μ_e. It is important that these two surfaces intersect, which is not the case for most of the other models [8]. In this case one can construct a MP connecting the pure phases along the intersection line. The thick curve on the surfaces shows pressure of charge neutral matter in β-equilibrium. The lower part of this curve (from low pressure to point C) corresponds to the pure HP. The MP starts at point C corresponding to baryonic density $\rho_B \simeq 1.5\,\rho_0$, and ends at point D corresponding to $\rho_B \simeq 5.1\,\rho_0$. At higher densities the matter is composed purely of quarks. Our calculations show that at $B^{1/4} > 190$ MeV the pressure surfaces of the HP and QP do not intersect at all and the MP can not be defined by the Gibbs rules.

The particle composition in these three regions is presented in Fig. 2. It is interesting to note that the only hyperon species which survive in the MP is Λ-particle which appears at densities $2.8\rho_0 < \rho_B < 5.1\rho_0$. All the negatively charged hyperons are suppressed as a result of the charge neutrality. The strangeness content of matter rapidly grows in the MP and reaches the asymptotic value of 1/3 in the QP. On the other hand, leptons (mainly electrons) are practically extinguished at $\rho_B \gtrsim 3\rho_0$.

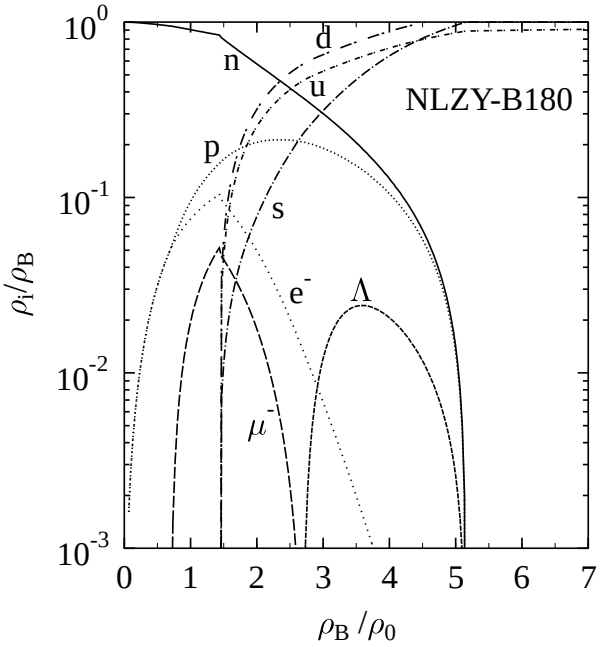

Figure 2: Relative particle abundances versus baryon density ρ_B as predicted by the combined NLZY and MIT Bag ($B^{1/4} = 180$ MeV) models. The region $1.5 < \rho_B/\rho_0 < 5.1$ corresponds to the mixed phase.

3 Properties of compact stars

Below we study properties of static spherically symmetric stars. Under assumption that the matter may be treated as an ideal fluid, the star structure can be found by solving the TOV equations [14]. For a given EoS, $P = P(\epsilon)$, and a fixed central baryon density $\rho_c = \rho_B(r = 0)$ we integrate the TOV equations from the center of the star up to its surface $r = R$. The star radius R is determined from the condition $P(R) = 0$. The details of numerical calculation as well as the online program can be found on the internet home page [15] of one of the authors (M.H.).

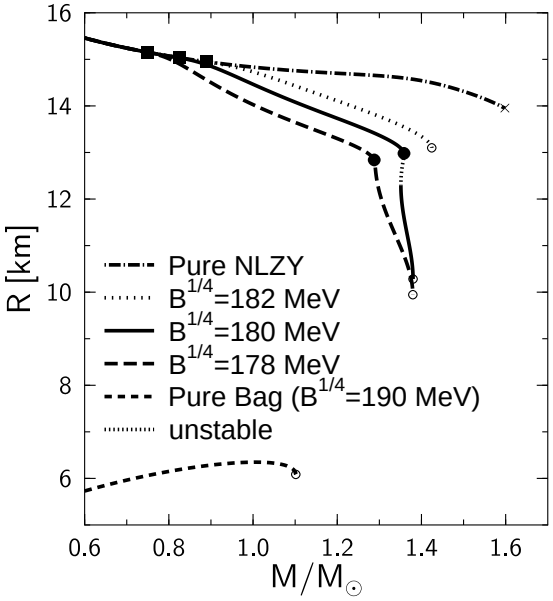

Figure 3: The mass-radius relations for different families of stars. Open dots correspond to the maximum mass. The beginning and the end of the mixed phase in hybrid stars are shown by full squares and dots.

In Fig. 3 we present the mass–radius relations calculated for several values of B as well as for pure hadronic and quark stars. By open dots we show the critical configurations with highest possible masses. The pure hadronic curve are calculated assuming the NLZY EoS at all densities. The part of this curve corresponding to $M > 1.6M_\odot$ is omitted due to appearance of densities with negative effective masses of baryons [12]. The beginning of the MP at the star center is marked by full squares whereas its end and, therefore, the beginning of the pure QP, is marked by full dots. As seen in Fig. 3, the model predictions depend strongly on the bag constant. Stable hybrid stars are possible only for low bag constants, $B^{1/4} \leq 180$ MeV. For higher B stars become unstable even before they reach high enough density for the formation of a pure deconfined phase in their interiors. On

the other hand, pure quark stars are possible at any B.

A very interesting feature is found in a narrow interval of B around $B^{1/4} = 180$ MeV, where a second sequence of stable hybrid stars appears. Their properties can be summarized as follows:

- The first sequence of stars can only reach maximum central baryon densities of about 0.77 fm^{-3} which is just at the end of the MP. As one can see from Fig. 3, stars of this sequence have masses below $M_{\max} = 1.36\,M_\odot$ and radii $R > 13$ km. These stars are mainly composed of hadronic and MP matter with admixture of the Λ-hyperons. The calculation shows that stars near the maximum mass contain a tiny core of pure quark phase.

- Stars of the second sequence have considerably higher central densities, $0.9\,\mathrm{fm}^{-3} < \rho_c < 1.53\,\mathrm{fm}^{-3}$. Their masses lies in a narrow interval, $1.35 < M/M_\odot < 1.38$ and their radii are noticeably smaller, $10.2\,\mathrm{km} < R < 12.3\,\mathrm{km}$. These stars are mainly composed of quark and MP matter, surrounded by a rather thin layer of HP and the nuclear crust.

- The two sequences of compact stars are separated by unstable region corresponding to the interval of central densities $0.78\,\mathrm{fm}^{-3} < \rho_c < 0.9\,\mathrm{fm}^{-3}$.

From our more comprehensive study [8] involving many other models of EoS we conclude that two sequences of compact stars, sometimes called twin stars, appear only in very exceptional cases. There is no guarantee that this picture is the one that corresponds to the reality. But we find it interesting to study its possible consequences for the dynamics and observable signatures of compact stars.

4 The twin star collapse

One can imagine the situation when a compact star on the first sequence has a mass close to $M_{\max}$. If this star is a member of binary system, then its mass and, therefore, its central density may grow due to accretion from a companion star. Eventually the mass will exceed the maximum value when the star becomes unstable with respect to radial compression. Usually it is assumed that this loss of stability leads to the collapse into a black hole. However, our calculations open another possibility: the collapse into the twin star on the second sequence.

Let us assume that no matter is ejected during this process, i.e. the total baryon number, N_B is conserved. Figure 4 shows the gravitational mass of the star as a function of its total baryon number. The star from the first sequence which reaches the maximum mass

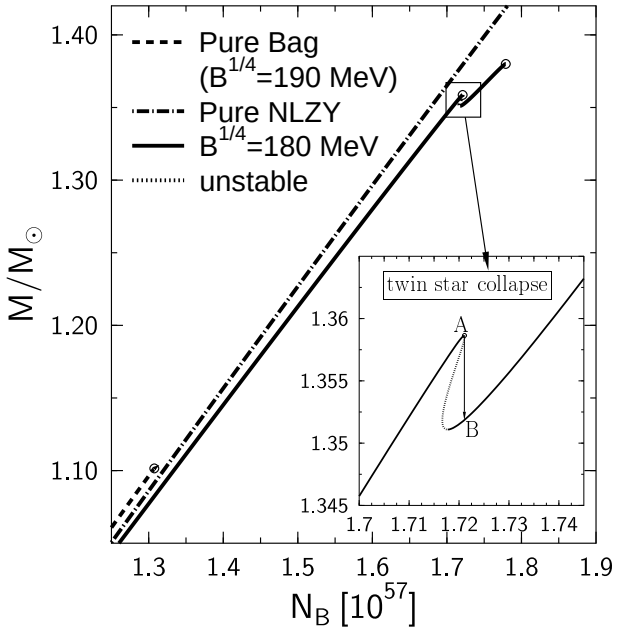

Figure 4: Mass as a function of baryon number for different families of stars. The inset shows the enhanced region of twin stars. The twin star collapse corresponds to the transition from A to B.

(point A) will collapse to its twin star. The latter is the corresponding star on the second sequence, i.e. the one which has the same total baryon number (point B). The difference in energy between these two stars, ΔE, is given by the difference in their gravitational masses. In the case considered here, the released energy is $\Delta E \simeq 6 \times 10^{-3} M_\odot \simeq 10^{52}$ erg. This amount of energy should finally be emitted in one or the other way.

The baryonic density profiles of the twin stars A and B are compared in Fig. 5. One can see that an extended MP is present in both cases but the star B has much larger quark core as compared to the star A, where this core is only marginally present. So, the instability develops practically at the end of the MP region. In other words, this shows that stars with small quark cores are unstable. In the considered example the new equilibrium state appears only when the core radius exceeds about 4 km. This reminds the well known result from the theory of nonrelativistic stars with a density jump inside. Namely, if ρ_1 and ρ_2 are baryon densities just below and above this jump, then small dense core becomes unstable if ρ_1/ρ_2 is larger than a certain critical value (3/2 for incompressible matter [16]). Of course, in our case there appears no jumps of density, although its gradients are large near the core boundary.

This kind of instability associated with a first order phase transition in hadronic matter was first studied in Ref. [17] and later on in Refs. [18, 19]. It was shown that the transition

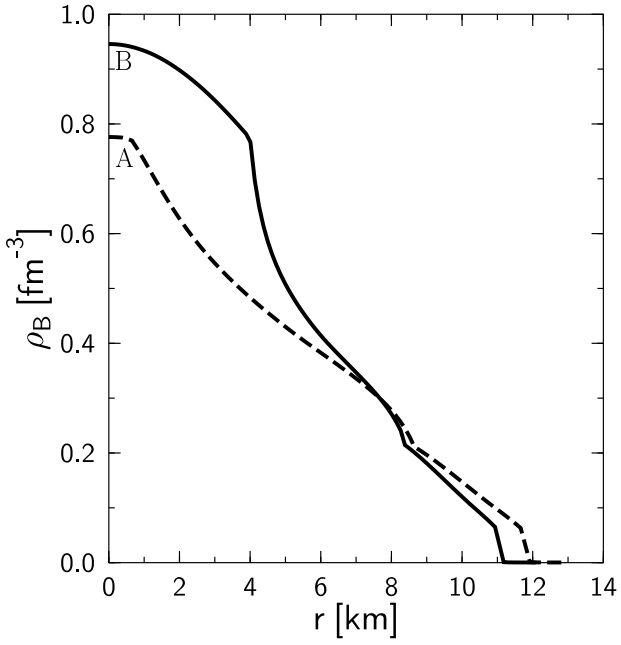

Figure 5: Baryon density profiles of the twin stars A and B as defined in Fig 4.

from a small-core to a large-core configuration proceeds via large-scale damped oscillations around the new equilibrium state. We expect that the collapse of twin stars may proceed in a similar way. After reaching the critical state A the star looses stability and enters the stage of catastrophic rearrangement. Since the QP in the core has higher density than the replaced MP, surrounding layers of the star will acquire collective inward motion. Due to inertial effects, the star will overshoot the new equilibrated state B and rebound. This will give rise to the damped oscillations around this state. As simple dimensional estimates show [17], the initial implosion and following oscillations are characterized by the millisecond time scale.

Such star rearrangement may involve many interesting processes. First of all, large amount of hadronic matter will be transformed into deconfined phase. Since strangeness and leptonic contents are very different in two phases, this transformation will require not only strong-interaction reactions but also weak processes changing strangeness and lepton numbers. Such reactions will inevitably produce large numbers of neutrinos. For instance, to achieve chemical equilibrium in the deconfined phase one needs reactions $e + u \to d + \nu$ and $u + d \to s + u$ which lead, respectively, to emission of neutrinos and production of additional strange quarks. We believe that the time scales of these weak

processes are much shorter than the characteristic times of the star collapse.

The total number of neutrinos, N_ν, produced during the transition process can be estimated as follows. From Fig. 5 one can see that the final star has the quark core with baryon density $\rho_{\rm core} \sim 5\rho_0$ and radius $R_{\rm core} \simeq 4$ km. Thus, the core contains $N_{\rm core} \sim 2 \times 10^{56}$ baryons. They were initially in the HP at lower density $\rho_B \sim 2\rho_0$. According to Fig. 2 the fraction of electrons in this phase was about 10% and practically no electrons were in the QP. Therefore, the difference between the number of electrons in configurations A and B is $\Delta N_e \sim 2 \times 10^{55}$ (the direct numerical calculation gives $\Delta N_e = 1.6 \times 10^{55}$). Because of lepton number conservation, all these electrons should be transformed into neutrinos and therefore, $N_\nu = \Delta N_e \sim 2 \times 10^{55}$. This number is about 1% of the total baryon number of the star $N_B \simeq 1.7 \times 10^{57}$. The neutrino energies will cover a broad range up to a maximum value $E_\nu^{\rm max} = \mu_e + \mu_u - \mu_d$. One can estimate $E_\nu^{\rm max}$ by assuming that initially the deconfined phase was produced in the nonequilibrium state with the flavor composition corresponding to the HP. The latter consisted mainly of neutrons, with the quark structure udd, as well as about 10% admixture of protons and electrons. Taking $\rho_d \simeq 2\rho_u \simeq 10\rho_0$ and $\rho_e \simeq 0.5\rho_0$ we get $E_\nu^{\rm max} \simeq 150$ MeV which corresponds to the mean neutrino energy ~ 100 MeV. Multiplying this energy by N_ν one obtains that a significant fraction ($\gtrsim 30\%$) of the released energy will be carried away by the prompt neutrino burst.

We expect that the remaining energy will be transformed into heat. Nonequilibrium processes during the phase transformation as well as viscosity effects might be responsible for dissipation of collective kinetic energy and eventually for damping of oscillations. Assuming that thermal energy ΔE_T is initially dissipated in the quark core, one can estimate its temperature T_0 from the relativistic Fermi gas formula

$$\frac{\pi^2}{4}\frac{T_0^2}{\mu_q} = \frac{\Delta E_T}{3N_{\rm core}}\,, \tag{13}$$

where $\mu_q = \mu_b/3 \simeq 0.4$ GeV is typical quark chemical potential at $\rho_B \sim \rho_{\rm core}$. For $\Delta E_T \sim 7 \times 10^{51}$ erg Eq. (13) gives $T_0 \simeq 40$ MeV. At later times the heat wave will propagate through the whole star and finally will produce photons and, possibly, electron-positron pairs at its surface. The emission temperature, $T_{\rm em}$, can be estimated by assuming that the thermal energy is distributed over the whole stellar matter, which is nonrelativistic outside the core. Then one obtains $T_{\rm em} \sim 2\Delta E_T/3N_B \sim 2$ MeV. These predictions give us a ground to think that the discussed mechanism may serve as the engine for Gamma-Ray Bursts (GRB) [20]. Another obvious prediction is that the discussed rearrangement of the star will lead to a significant change in its moment of inertia. In a rotating star this will result in a super-glitch phenomenon [21].

5 Conclusions and outlook

It is shown that within a realistic hybrid (NLZY-MIT Bag) model two sequences of compact stars (twin stars) are possible. We demonstrate that their interiors differ mainly by the size of pure quark core. The energy difference between two twin stars with the same baryon number is about 10^{52} erg which is approximately 1% of their total energy. The transition between twin stars may be triggered by accretion of mass from a companion star or by some other processes leading to increase of the central density above the critical value. After that a catastrophic rearrangement of the star begins. It will first collapse and then oscillate around a new equilibrium state.

Our estimates show that in the course of this process the quark core can be heated up to temperature of about 40 MeV which is comparable to the one in supernova explosions. Our main prediction is that the transition between twin stars will produce a prompt burst of neutrinos (with energies of about 100 MeV) followed by a gamma ray burst (with photon energies of about 1 MeV). These features of the twin star collapse make it a potential candidate for the GRBs. On the other hand, there are some characteristics of GRBs, e.g. beaming of radiation, which is impossible to explain without additional assumptions invoking rotation and strong magnetic fields. This problem needs further study.

It is interesting to note that the presented model predicts maximum masses of compact stars, $(1.35 - 1.38)M_{\odot}$, which agree well with observed masses of pulsars [3]. Moreover, the twin stars of the second sequence have nearly the same masses in the broad range of ρ_c. If pulsars have quark cores, this may explain why their measured masses are clustered near the mass of about $1.4M_{\odot}$.

Other phase transitions may take place in the interiors of compact stars, e.g. kaon condensation, color superconductivity etc. In Ref. [6] it was shown that formation of metastable hyperonic matter can also lead (in a certain range of parameters) to the twin star solutions. The comparison of twin star properties predicted by different models will be given in a separate work [8].

Acknowledgements

The authors thank J. Schaffner–Bielich for fruitful discussions. This work was funded in part by GSI, DAAD, DFG and the Hessische Landesgraduiertenförderung. A.B. thanks the Alexander von Humboldt Foundation for support. I.N.M. and L.M.S. acknowledge support from the RFBR Grant No. 00–15–96590.

References

[1] M. Rufa, P.-G. Reinhard, J. Maruhn, W. Greiner, and M.R. Strayer, Phys. Rev. C **38**, 390 (1988).

[2] A. Chodos, R.L. Jaffe, K. Johnson, C.B. Thorn, and V.F. Weisskopf, Phys.Rev. D **9**, 3471 (1974).

[3] N.K. Glendenning, *Compact Stars* (Springer, New York, 1997).

[4] A.W. Steiner, M. Prakash, and J.M. Lattimer, Phys. Lett. B **486**, 239 (2000).

[5] M. Hanauske, L.M. Satarov, I.N. Mishustin, H. Stöcker, and W. Greiner, Phys. Rev. D **64**, 043005 (2001).

[6] J. Schaffner-Bielich, M. Hanauske, H. Stöcker, and W. Greiner, Phys. Rev. Lett. **89**, 171101 (2002).

[7] G.F. Burgio, M. Baldo, P.K. Sahu, and H.J. Schulze, Phys.Rev. C **66**, 025802 (2002).

[8] M. Hanauske, A. Bhattacharyya, L.M. Satarov, I.N. Mishustin, H. Stöcker, and W. Greiner, to appear on astro-ph.

[9] U.H. Gerlach, Phys. Rev. **172**, 1325 (1968).

[10] N.K. Glendenning, C. Kettner, astro-ph/9807155; Astron. Astrophys., **353**, L9 (2000).

[11] K. Schertler, C. Greiner, J. Schaffner-Bielich, and M.H. Thoma, Nucl.Phys. A **677**, 463 (2000).

[12] J. Schaffner and I. Mishustin, Phys. Rev. C **43**, 1416 (1996).

[13] N.K. Glendenning, Phys. Rev. D **46**, 1274 (1992).

[14] R.C. Tolman, Phys. Rev. **55**, 364 (1939); J.R. Oppenheimer and G.M. Volkoff, *ibid* **55**, 374 (1939).

[15] *http://www.th.physik.uni-frankfurt.de/∼hanauske/index.html*

[16] W.H. Ramsey, Mon. Not. R. Astron. Soc. **110**, 325 (1950); M.J. Lighthill, *ibid* **110**, 339 (1950).

[17] A.B. Migdal, A.I. Chernoutsan, and I.N. Mishustin, Phys. Lett. **83B**, 158 (1979).

[18] B. Kämpfer, Phys. Lett. **101B**, 366 (1981).

[19] P. Haensel, J.L. Zdunik, and R. Schaeffer, Astron. Astrophys. **217**, 137 (1989).

[20] T. Piran, Phys. Rep. **333-334**, 529 (2000).

[21] F. Ma and B. Xie, Astrophys. J. **462**, L63 (1996).